Particle Accelerators, 1987, Vol. 22, pp. 129–147
Photocopying permitted by license only

Printed in the United States of America

SYNCHRONIZED PERIODIC ORBITS IN BEAM–BEAM INTERACTION MODELS OF ONE AND TWO SPATIAL DIMENSIONS

TASSOS C. BOUNTIS†
Department of Mathematics, University of Patras, Patras, Greece

GAMAL M. MAHMOUD
Department of Mathematics and Computer Science, Clarkson University, Potsdam, NY 13676

(Received August 1, 1986; in final form January 23, 1987)

Analytical and numerical methods of nonlinear dynamics are used to study some simple periodic solutions (or orbits) of differential equation models of the beam–beam interaction in one and two spatial dimensions. These periodic orbits are called *synchronized* because their frequencies $\omega_i = n_i/m_i$, $i = 1, 2$, are very nearly equal to the unperturbed ("betatron") frequencies, or "tunes," Q_i, in the horizontal and vertical directions (n_i, m_i are small positive integers). They correspond to some of the lowest-order *resonances* of the system and are experimentally important because, when they come close enough to the origin of phase space, they can carry particles away from their ideal path, causing serious beam blowup effects. In this paper, we obtain such synchronized periodic orbits by numerical as well as analytical techniques and determine their stability properties by perturbative methods, for large ranges of parameter values and initial conditions. Our results also demonstrate interesting qualitative and quantitative similarities between differential and difference equation models of colliding proton beams in two spatial dimensions.

1. INTRODUCTION

In recent years, there has been an increased interest in the applications of the methods and techniques of nonlinear dynamics to the problem of colliding particle beams in high-energy accelerators.[1–3] One of the most important aspects of this problem is the question of stability of particle orbits, since the two beams repeatedly intersect, imparting on one another an instantaneous, electromagnetic "kick," referred to here as the beam–beam interaction. These kicks are caused by strongly nonlinear forces, which, since the beams often have to intersect as many as 10^{11} times (!) before an interesting "collision" is observed, can have disastrous effects, e.g., severe beam blowup and particle loss to the walls of the machine.

The dynamics of the beam–beam interaction is governed by *resonances*[1,2] (or simple periodic orbits), which can "trap" particles in their stability region and

† On leave from the Department of Mathematics and Computer Science, Clarkson University, Potsdam, NY 13676

take them dangerously far from the ideal beam path (passing by the origin of the phase space of the system). The main objective here, therefore, is to locate these resonances and study their stability regions, so as to be able to estimate the phase-space distances to which they may take particles away from the origin.[4–6]

One way to approach this problem is to consider beam–beam interaction models in the so-called weak-strong approximation, in which the particles of one non-self-interacting (weak) beam are taken to collide head-on, with a bunched strong beam, whose (cumulative) electromagnetic effect can be described by the Hamiltonian[1–6]

$$H = \tfrac{1}{2}(\dot{x}^2 + \dot{y}^2 + Q_1^2 x^2 + Q_2^2 y^2) + \delta_{2\pi}(t) B V(x, y). \tag{1}$$

Here, x and y are the horizontal and vertical displacements of the weak-beam particle from its ideal (circular) path, Q_1, Q_2 are the so-called machine tunes, or betatron (unperturbed) oscillation frequencies, B measures the strength of the beam–beam interaction potential $V(x, y)$, and $\delta_{2\pi}(t)$ is the 2π-periodic delta function representing the extremely short duration of the interaction:[1–6]

$$\delta_{2\pi}(t) = \sum_{n=-\infty}^{\infty} \delta(t - 2\pi n) = \frac{1}{2\pi} \sum_{n=-\infty}^{\infty} \cos nt. \tag{2}$$

The Hamiltonian formulation of the problem, Eq. (1), implies that we are dealing with the conservative, proton beam case,[4,5] even though radiation damping can always be included in our models[6] and treated by techniques similar to the ones described in this paper. Using now for our beam–beam interaction force an expression derived for a strong beam with a Gaussian cylindrically symmetric charge distribution,[7]

$$\frac{1}{x}\frac{\partial V}{\partial x} = \frac{1}{y}\frac{\partial V}{\partial y} = 2\frac{1 - \exp[-(x^2 + y^2)/2]}{x^2 + y^2} = 1 - \frac{x^2 + y^2}{4} + O(|x^2 + y^2|^2), \tag{3}$$

we arrive, from all of the above, at the equations of motion

$$\ddot{x} + Q_1^2 x + \frac{B}{4\pi}\left(\frac{1}{2} + \cos t + \cdots\right)\left[x - \frac{x(x^2 + y^2)}{4} + \cdots\right] = 0, \tag{4a}$$

$$\ddot{y} + Q_2^2 y + \frac{B}{4\pi}\left(\frac{1}{2} + \cos t + \cdots\right)\left[y - \frac{y(x^2 + y^2)}{4} + \cdots\right] = 0. \tag{4b}$$

In this paper, we shall be interested in obtaining analytically, as well as numerically, some fundamental periodic solutions of Eq. (4), in one and two spatial dimensions, with frequencies $\omega_i = n_i/m_i \cong Q_i$, $i = 1, 2$ (n_i, m_i are positive integers). These so-called synchronized periodic orbits are important, because they correspond to some of the lowest-order resonances[1,2,5] of the system. When they are *stable* (with respect to small perturbations in their initial conditions), they turn out to have *large* regions around them where the solutions of Eq. (4) behave in a more-or-less predictable way: In the one-dimensional case [$x(t) \equiv 0$, say, for all t, in Eq. (4)], most orbits are bounded by invariant tori[1–4] for all time, while, when both x and y are involved, significant blowup phenomena are observed as orbits "diffuse," through a network of resonances, to more and more distant regions of phase space.[5,6]

We have recently introduced a novel numerical technique for finding such synchronized periodic orbits and have used perturbative methods to study them analytically in periodically driven nonlinear oscillators.[8] Here, these methods are applied first to a differential equation like Eq. (4b), in one spatial dimension,[9]

$$\frac{d^2y}{dt^2} + ay + \varepsilon \cos 2t(y - by^3) = 0, \tag{5}$$

for which synchronized periodic solutions are discovered numerically in Section 2, with $\sqrt{a} \cong 1,\ 1/2,\ b = 1$, and $0 < \varepsilon \leq 1.0$. These solutions are also obtained analytically by the method of generalized averaging[10] (to order ε^2) in Section 3. The results of Section 3 are then used in a stability analysis of these solutions, carried out here with the aid of multiple scaling perturbation techniques.[11] Excellent agreement is found between theoretical predictions and numerical computations, over large ranges of parameter values and initial conditions.

The main methods and results of this paper are not affected by the precise form of the parametric driving force in our equations, as long as it is *periodic* in *t*. Thus, the addition of more cosines in the coefficient of the beam–beam force in Eq. (5), cf. Eq. (4), is seen not to change our analysis and its main outcome significantly. However, in an effort to make our results of greater qualitative and quantitative relevance to the beam–beam interaction problem, we have in Section 4, extended and applied our methods to the more realistic two-dimensional system

$$\ddot{x} + Q_1^2 x + \varepsilon(\tfrac{1}{2} + \cos t + \cos 2t + \cos 3t)\left[x - \frac{x(x^2+y^2)}{4}\right] = 0, \tag{6a}$$

$$\ddot{y} + Q_2^2 y + \varepsilon(\tfrac{1}{2} + \cos t + \cos 2t + \cos 3t)\left[y - \frac{y(x^2+y^2)}{4}\right] = 0. \tag{6b}$$

Cf. Eq. (4) above. Extending the techniques of generalized averaging, we obtained approximate formulas for curves in the Q_1, ε and Q_2, ε planes, with $Q_1 \cong 3/4$, $Q_2 \cong 1/2$, along which Eqs. (6) possess synchronized periodic solutions with periods $T_1 = 8\pi/3$ and $T_2 = 4\pi$, respectively (i.e., overall period $T = 8\pi$). These formulas were tested numerically and found to be quite accurate for $0 < \varepsilon \lesssim 0.2$.

The particular choice of the unperturbed frequencies Q_1 and Q_2 mentioned above (i.e., $Q_1 \cong 3/4$, $Q_2 \cong 1/2$) yields, of course, a whole multiplet of resonances

$$m_1(\tfrac{3}{4}) + m_2(\tfrac{1}{2}) = m_1 Q_1 + m_2 Q_2 = n, \tag{7}$$

(m_1, m_2, n integers; m_1, n nonnegative), which can now be examined in greater detail using the results of this paper. Clearly, the lowest-order ones among them (for which m_1, m_2 are smallest in magnitude) are expected to be the most important.[1,2,4,5]

We have started such an analysis here by taking $m_2 = 0$, $m_1 = 4$ ($n = 3$), a familiar case from some of our earlier investigations.[4–6] The pictures we obtained of orbits intersecting the x, $\dot{x}$ (and y, $\dot{y}$) planes at integer multiples of 2π bear a striking resemblance to similar ones produced by iterating mapping models of the beam–beam interaction[4,5]! Thus, further comparisons between differential and difference equation studies of colliding beams are currently under investigation, and a more comprehensive resonance analysis of this problem, using synchronized periodic orbits, will appear in future publications.

2. A NUMERICAL INVESTIGATION OF PERIODIC ORBITS

In this section, we apply a novel numerical technique for finding periodic solutions of differential equations of the form

$$\frac{d^2y}{dt^2} + ay + \varepsilon P(\Omega t)F(y) = 0, \qquad P(\Omega t) = P(\Omega t + 2\pi), \tag{8}$$

to the nonlinear Mathieu equation

$$\frac{d^2y}{dt^2} + ay + \varepsilon \cos 2t(y - by^3) = 0, \qquad b \geq 0, \tag{9}$$

whose connection to the problem of colliding beams has been discussed in the introduction, as well as in Refs. 1 and 2. The parameter ε is taken to be small, but good agreement between numerical and analytical results is generally obtained for $|\varepsilon| \lesssim 1.0$.

As is the case with the *linear* Mathieu equation[12] the $\cos 2t$ in Eq. (9) is the major resonance-producing term to lowest order in a perturbation approach in powers of ε. Near these lowest-order resonances, the solutions oscillate with unperturbed frequency squared,

$$a = p^2 + \varepsilon a_1 + \varepsilon^2 a_2 + \cdots, \tag{10a}$$

where

$$p = 0, \tfrac{1}{2}, 1, \tfrac{3}{2}, 2, \ldots. \tag{10b}$$

Using our so called *indicatrix method*, we shall determine numerically the values of the parameters a, ε at which periodic orbits of Eq. (9) with frequency $p \approx \sqrt{a}$ pass by a specified initial condition, e.g., $[y(t_0), \dot{y}(t_0)] = (0.5, 0)$.

Clearly, for $\varepsilon = 0$, all points $[y(t_0), \dot{y}(t_0)]$ can serve as initial conditions for periodic orbits with frequency $p \cong \sqrt{a}$. However, for $\varepsilon \neq 0$, the set of points $[y(t_0 + T), \dot{y}(t_0 + T)]$ with $T = 2\pi/p$ form a closed curve parametrized by $t_0 \in [0, \pi]$ that may or may not pass by our specified initial condition $(0.5, 0)$. This closed curve is called the *indicatrix* and is plotted here in Fig. 1a for $a \cong 1/4$ in Eq. (9) (and $b = 1$).

By varying slightly a and ε, we obtain the desired periodic orbits when the indicatrix is observed to pass by our initial condition at some values of t_0. This can happen, of course, for more than one value of $t_0 \in [0, \pi]$; see Figs. 1b and 1c, where $t_0 = 0$ and $\pi/2$, respectively.

We consider here the cases $p = 1$ and $p = 1/2$ (other values of p can be similarly

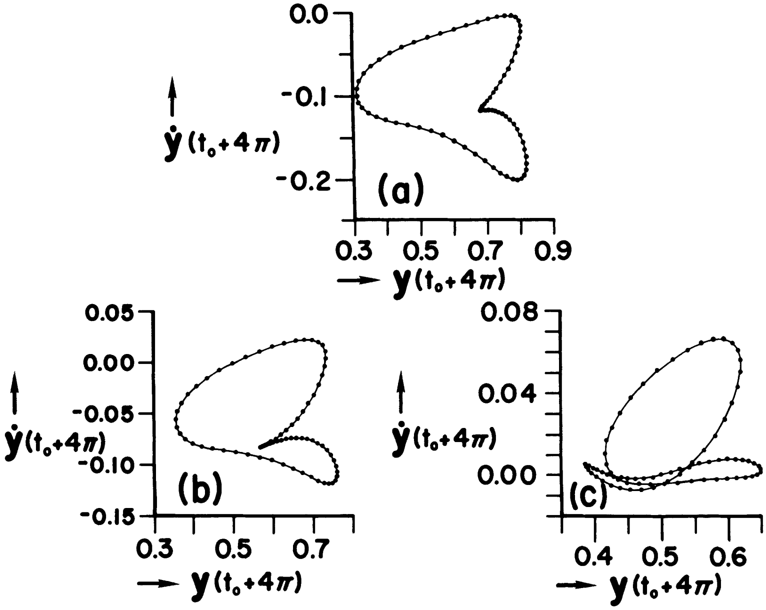

FIGURE 1 Indicatrix plots of Eq. (9) for $\varepsilon = 0.6$, $b = 1$, and $t_0 \in [0, \pi]$ for (a) $a = 0.251213$, (b) $a = 0.2359465$ [note: $(0.5, 0)$ at $t_0 = 0$], (c) $a = 0.2124235$ [$(0.5, 0)$ at $t_0 = \pi/2$].

treated), and we study in this way the existence of these so-called synchronized periodic solutions with periods $T = 2\pi,\ 4\pi$, respectively. We find, with our indicatrix method, *two* curves in the $a,\ \varepsilon$ plane corresponding to periodic orbits with $t_0 = 0,\ \pi/2$; see Fig. 2.

To examine these periodic orbits in more detail we use the Poincaré map associated with Eq. (9), at the parameter values suggested by the indicatrix method. In fact, using the Poincaré map one can even determine the *stability properties* of these periodic solutions under small perturbations in the initial conditions. We illustrate this below for the cases $p = 1,\ 1/2$ (or $a \cong 1,\ 1/4$).

Let us consider the Poincaré map, or the $y,\ \dot{y}$ surface of section $\Sigma^{t_0} = \{[y(t_n), \dot{y}(t_n)],\ t_n = t_0 + n\pi\}$. We know from the Poincaré–Birkhoff fixed-point theorem[13,14] that for $\varepsilon \neq 0$ the invariant curves corresponding to periodic orbits of the $\varepsilon = 0$ case break up into an even number of periodic orbits, half of which are *stable* (elliptic) and half *unstable* (hyperbolic).

On the other hand, it is also possible for a *single* periodic orbit to appear on a surface of section after a *bifurcation* from an orbit with half its period, at some value of a parameter of the problem.[13,15] Upon such an event, the "mother" orbit destabilizes, while the new orbit is "born" (linearly) stable to small changes in its $y(t_0)$ and $\dot{y}(t_0)$.

Integrating Eq. (9) numerically for $a \cong 1$ ($b = 1$) and several initial conditions and plotting the intersections of orbits on the $y,\ \dot{y}$ surface of section of Fig. 3, we find that the latter case occurs for this choice of parameters: In other words, our indicatrix method has picked *a single period-*2π orbit, intersecting the y axis at $(-0{\cdot}5, 0)$ and $(0.5, 0)$ (see Fig. 3a for $t_0 = 0$ and Fig. 3b for $t_0 = \pi/2$). This orbit

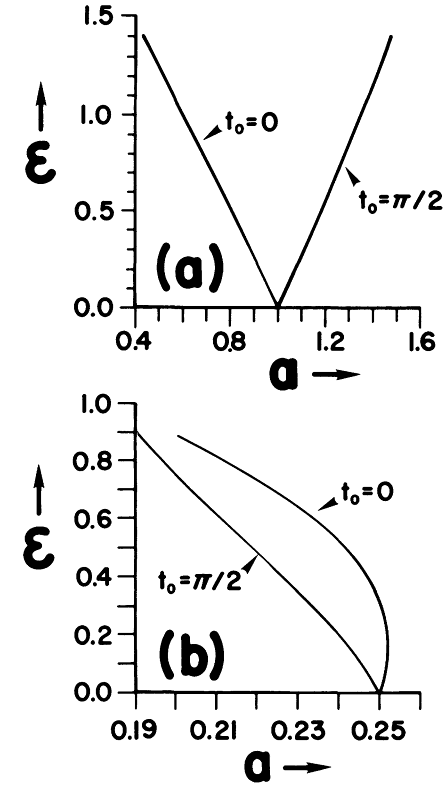

FIGURE 2 Synchronized periodic solutions of Eq. (9) with period (a) $T = 2\pi$, (b) $T = 4\pi$.

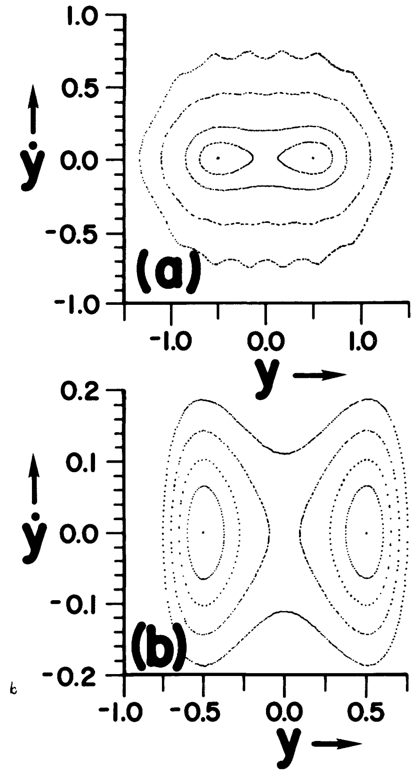

FIGURE 3 Surfaces of section for Eq. (9) for $\varepsilon = 0.5$, $b = 1$ and (a) $a = 0.80674575$, $t_0 = 0$, (b) $a = 1.181495$, $t_0 = \pi/2$. Clearly, in this case, the two curves of Fig. 2a yield the same orbit.

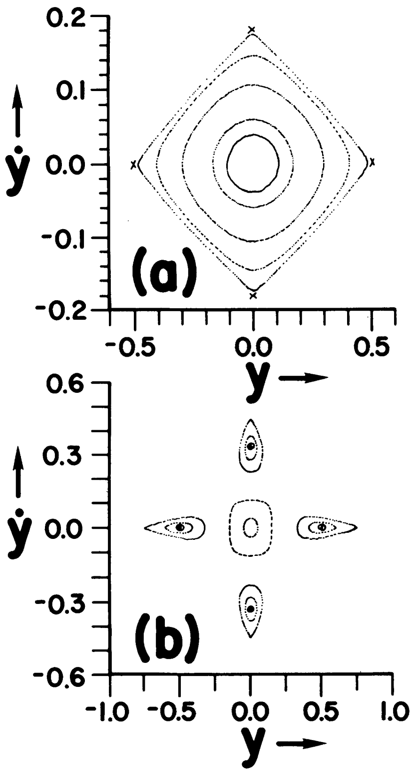

FIGURE 4 Surfaces of section for Eq. (9) for $\varepsilon = 0.6$, $b = 1$ and (a) $a = 0.2359465$, $t_0 = 0$ (the unstable period-4π orbit marked by x), (b) $a = 0.212435$, $t_0 = \pi/2$ (the stable period-4π orbit, marked by $\odot$).

has actually bifurcated at $\varepsilon = 0$ out of the origin, which for $\varepsilon > 0$ becomes an (unstable) orbit of period π.

In the case $p = 1/2$ ($a \cong 1/4$), however (where the origin is a stable period-π orbit), there are *two* periodic orbits of period 4π, which fall within the class described by Birkhoff's theorem; i.e., one of them is unstable (see Fig. 4a at $t_0 = 0$) and the other stable (see Fig. 4b at $t_0 = \pi/2$).

3. SYNCHRONIZED PERIODIC ORBITS: A THEORETICAL STUDY IN ONE DIMENSION

Using the method of generalized averaging,[10] we can derive first- and second-order (in ε) analytical formulas for synchronized periodic solutions of the nonlinear Mathieu equation

$$\frac{d^2y}{dt^2} + ay + \varepsilon \cos 2t(y - by^3) = 0, \qquad b \geq 0 \tag{11}$$

and compare them with the numerical results obtained by the indicatrix method of Section 2.

Introducing the new variables

$$Y \equiv y\sqrt{b}, \qquad \omega^2 \equiv a, \tag{12}$$

we first rewrite Eq. (11) as

$$\frac{d^2Y}{dt^2} + \omega^2 Y + \varepsilon \cos 2t(Y - Y^3) = 0. \tag{13}$$

When $\varepsilon = 0$, the general solution of Eq. (13) is

$$Y(t) = a \cos(\omega t + \phi), \ \dot{Y}(t) = -a\omega \sin(\omega t + \phi), \ a, \ \phi \ \text{const.} \tag{14}$$

For $\varepsilon \neq 0$, but "small enough," we shall allow a and ϕ to be unknown functions of t in Eq. (14), which are to be determined below, to second order in ε.

Differentiating the first equation of Eq. (14) and equating with the second and differentiating the second of Eq. (14) and substituting into Eq. (13), we get a system of equations that we solve for $\dot{a}(t)$ and $\dot{\phi}(t)$ to obtain

$$\frac{d}{dt}\begin{bmatrix} a(t) \\ \phi(t) \end{bmatrix} = \frac{\varepsilon}{4\omega}\begin{bmatrix} a(t)(\sin\psi_1 + \sin\psi_2) \\ \cos\psi_1 + \cos\psi_2 + 2\cos 2t \end{bmatrix}$$

$$- \frac{\varepsilon a^2(t)}{16\omega}\begin{bmatrix} a(t)(2\sin\psi_1 + 2\sin\psi_2 + \sin\psi_3 + \sin\psi_4) \\ 4\cos\psi_1 + 4\cos\psi_2 + \cos\psi_3 + \cos\psi_4 + 6\cos 2t \end{bmatrix}, \tag{15a}$$

where the $\cos^3(\omega t + \phi)$ term has been expanded and

$$\begin{aligned} \psi_1 &= 2(\omega + 1)t + 2\phi(t), \qquad & \psi_2 &= 2(\omega - 1)t + 2\phi(t), \\ \psi_3 &= 2(2\omega + 1)t + 4\phi(t), \qquad & \psi_4 &= 2(2\omega - 1)t + 4\phi(t). \end{aligned} \tag{15b}$$

Now we attempt to solve the nonlinear Eq. (15a) with Eq. (15b) by the generalized averaging method as follows:

Casting the original Eq. (15) in the form

$$\frac{dz}{dt} = \varepsilon f(z, t), \qquad z = \begin{bmatrix} a(t) \\ \phi(t) \end{bmatrix}, \tag{16a}$$

and writing

$$f(z, t) = \bar{f}(x) + \tilde{f}(x, t), \qquad x = \begin{bmatrix} a(t_0) \\ \phi(t_0) \end{bmatrix} = \begin{bmatrix} A \\ \Phi \end{bmatrix}, \tag{16b}$$

where $\bar{f}(x)$ contains the constant terms and terms of smallest frequency and $\tilde{f}(x, t)$ the terms of higher frequency, one associates with Eq. (16) the following reduced system:

$$\frac{dx}{dt} = \varepsilon \bar{F}(x) \tag{17a}$$

with

$$z = x + \varepsilon \tilde{G}(x, t). \tag{17b}$$

Expanding $\bar{F}(x)$ and $\tilde{G}(x, t)$ as series in ε,

$$\bar{F}(x) = \bar{F}_1(x) + \varepsilon \bar{F}_2(x) + \cdots + \varepsilon^{m-1}\bar{F}_m(x) + \cdots \tag{18a}$$

$$\tilde{G}(x, t) = \tilde{G}_1(x, t) + \varepsilon \tilde{G}_2(x, t) + \cdots + \varepsilon^{m-1}\tilde{G}_m(x, t) + \cdots \tag{18b}$$

and substituting from Eq. (17b) into Eq. (16) using Eqs. (17a) and (18) yields upon equating like powers of ε:

$$\bar{F}_1(x) = \overline{\tilde{f}(x,t)}, \qquad \bar{F}_2(x) = \overline{\frac{\partial \tilde{f}}{\partial x} \int \tilde{f}(x,t)\,dt}, \ldots \tag{19a}$$

and

$$\left.\begin{aligned} \tilde{G}_1(x,t) &= \int \tilde{f}(x,t)\,dt, \\ \tilde{G}_2(x,t) &= \int \widetilde{\left[\frac{\partial \tilde{f}}{\partial x}\int \tilde{f}(x,t)\,dt\right]}dt + \frac{\partial \bar{f}}{\partial x}\int\left[\int \tilde{f}(x,t)\,dt\right]dt \\ &\quad - \left\{\int\left[\int \frac{\partial \tilde{f}}{\partial x}(x,t)\,dt\right]dt\right\}\bar{f}, \ldots \end{aligned}\right\} \tag{19b}$$

Note that Eq. (15) is split in such a way that small frequency components occur at $\omega \cong 1$, 1/2. This means that we can get periodic orbits with period 2π, 4π already by the first approximation. To find periodic orbits with period greater than 4π, we need to go to second- or higher-order approximations. The amplitude and phase of these orbits are written in the form of ε-series expansions as follows:

$$a(t) = A + \varepsilon\tilde{G}_{1a}(x,t) + \varepsilon^2\tilde{G}_{2a}(x,t) + O(\varepsilon^3) \tag{20a}$$

$$\phi(t) = \Phi + \varepsilon\tilde{G}_{1\phi}(x,t) + \varepsilon^2\tilde{G}_{2\phi}(x,t) + O(\varepsilon^3) \tag{20b}$$

where

$$\tilde{G}_1(x,t) = \begin{bmatrix} \tilde{G}_{1a}(x,t) \\ \tilde{G}_{1\phi}(x,t) \end{bmatrix}, \qquad \tilde{G}_2(x,t) = \begin{bmatrix} \tilde{G}_{2a}(x,t) \\ \tilde{G}_{2\phi}(x,t) \end{bmatrix},$$

cf. Eq. (16), and $\tilde{G}_1(x,t)$, $\tilde{G}_2(x,t)$ are to be solved from Eq. (19b) to obtain the periodic solutions of Eq. (13) to order ε, ε^2, etc.

We present here the analytical expressions for such periodic orbits with period 2π, up to second order in ε. Observe that when $\omega \cong 1$, the terms of smallest frequency are

$$\begin{aligned} \bar{F}_1(x) &= \overline{f(x,t)} = \begin{bmatrix} \overline{f_1(x,t)} \\ \overline{f_2(x,t)} \end{bmatrix} \\ &= \frac{1}{4\omega}\begin{bmatrix} A\sin(2(\omega-1)t+2\Phi) \\ \cos(2(\omega-1)t+2\Phi) \end{bmatrix} \frac{-A^2}{8\omega}\begin{bmatrix} A\sin(2(\omega-1)t+2\Phi) \\ 2\cos(2(\omega-1)t+2\Phi) \end{bmatrix}, \end{aligned} \tag{21a}$$

and those of higher frequency:

$$\begin{aligned} \tilde{f}(x,t) = \begin{bmatrix} \tilde{f}_1(x,t) \\ \tilde{f}_2(x,t) \end{bmatrix} &= \frac{1}{4\omega}\begin{bmatrix} A\sin\Psi_1 \\ \cos\Psi_1 + 2\cos 2t \end{bmatrix} \\ &\quad \frac{-A^2}{16\omega}\begin{bmatrix} A(2\sin\Psi_1 + \sin\Psi_3 + \sin\Psi_4) \\ 4\cos\Psi_1 + \cos\Psi_3 + \cos\Psi_4 + 6\cos 2t \end{bmatrix}, \end{aligned} \tag{21b}$$

where

$$\Psi_1 = 2(\omega+1)t + 2\Phi,\ \Psi_3 = 2(2\omega+1)t + 4\Phi,\ \text{and}\ \Psi_4 = 2(2\omega-1)t + 4\Phi. \quad (21c)$$

To derive the reduced system [Eq. (17a)] to second approximation, we need also to calculate the function $\bar{F}_2(x)$ from Eq. (19a), using Eqs. (21b) and (21c). This gives

$$\bar{F}_2(x) = \frac{A^2}{128\omega^2}\begin{bmatrix} 4A\sin(4(\omega-1)t+4\Phi) \\ 4\cos(4(\omega-1)t+4\Phi) \end{bmatrix} \frac{-A^4}{512\omega^2}\begin{bmatrix} 3A\sin(4(\omega-1)t+4\Phi) \\ \left(\frac{6}{2\omega-1}+12\right)\cos(4(\omega-1)t+4\Phi) \end{bmatrix}. \quad (22)$$

Using Eqs. (21a), (22), and (18a), we write our reduced system [Eq. (17a)] in the form

$$\frac{d}{dt}\begin{bmatrix} A \\ \Phi \end{bmatrix} = \varepsilon\bar{F}_1(x) + \varepsilon^2\bar{F}_2(x) + O(\varepsilon^3). \quad (23)$$

To satisfy the condition $\frac{dA}{dt} = 0$, we make the corresponding contributions of $\bar{F}_1(x)$ and $\bar{F}_2(x)$ vanish by choosing

$$2(\omega-1)t + 2\Phi = k\pi \qquad (k = 0,\ 1 \text{ for } 2\pi\text{-periodic orbits}). \quad (24)$$

Now the second equation of Eq. (23) [with $\omega - 1 = d\Phi/dt$, cf. Eq. (24)] yields

$$\omega = 1 + \frac{\varepsilon}{4\omega}[(-1)^{k+1} + A^2(-1)^k] + \frac{\varepsilon^2 A^2}{32\omega^2}\left[-1 + \frac{A^2}{16}\left(12 + \frac{6}{2\omega-1}\right)\right], \quad (25)$$

which provides us with approximate expressions for the curves in the (a, ε) plane obtained numerically in Section 2.

The $t_0 = 0$ $(k = 0)$ curve is

$$\omega^2 = 1 - \frac{\varepsilon}{2}(1-A^2) - \frac{\varepsilon^2}{16}(1-A^2)^2 - \frac{\varepsilon^2 A^2}{16}(1 - \tfrac{3}{2}A^2) + O(\varepsilon^3), \quad (26a)$$

while for $k = 1$ $(t_0 = \pi/2)$ the curve is

$$\omega^2 = 1 + \frac{\varepsilon}{2}(1-A^2) - \frac{\varepsilon^2}{16}(1-A^2)^2 - \frac{\varepsilon^2 A^2}{16}(1 - \tfrac{3}{2}A^2) + O(\varepsilon^3). \quad (26b)$$

Equations (26a) and (26b) are already in very good agreement with the curves computed directly by the indicatrix method; see Figs. 5a and 2a.

In order to determine the amplitude and the phase of these 2π-periodic orbits to obtain an approximate expression for the solution $\hat{Y}(t)$, we need to calculate the functions $\tilde{G}_1(x, t)$ and $\tilde{G}_2(x, t)$. Since the calculations quickly become very complicated, we will determine $\hat{Y}(t)$ only up to $O(\varepsilon^2)$. By substituting from Eq. (21b) into Eq. (19b) we obtain

$$\tilde{G}_1(x, t) = \begin{bmatrix} \tilde{G}_{1a}(x, t) \\ \tilde{G}_{1\phi}(x, t) \end{bmatrix}, \quad (27)$$

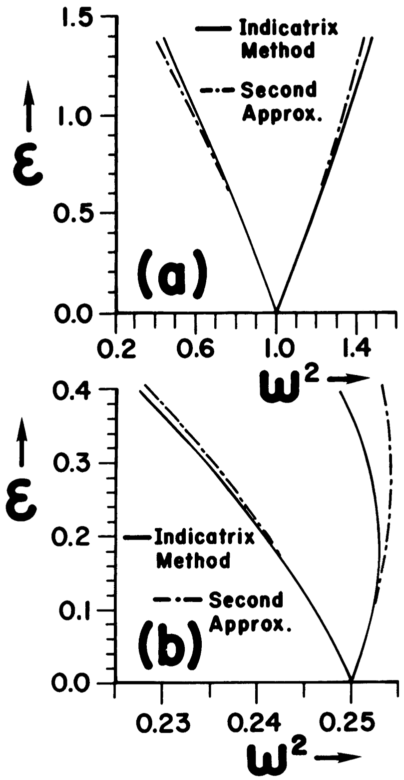

FIGURE 5 Comparison between the analytical formulas [Eqs. (26) and (30)] and the numerical results of Fig. 2.

where

$$\tilde{G}_{1a}(x, t) = \frac{-A}{16}\cos(4t + k\pi) + \frac{A^3}{16}[\tfrac{1}{6}\cos(6t + 2k\pi) + \tfrac{1}{2}\cos(4t + k\pi) + \tfrac{1}{2}\cos(2t + 2k\pi)] \tag{28a}$$

and

$$\tilde{G}_{1\phi}(x, t) = \tfrac{1}{16}[\sin(4t + k\pi) + 4\sin 2t] - \frac{A}{16}[\tfrac{1}{6}\sin(6t + 2k\pi) + \sin(4t + k\pi) + \tfrac{1}{2}\sin(2t + 2k\pi) + 3\sin 2t]. \tag{28b}$$

Substituting from Eq. (28) into Eq. (20) and using Eq. (24), we obtain the following analytical expression for $\hat{Y}(t)$ from Eq. (14):

$$\hat{Y}(t) = A\cos\left(t + \frac{k\pi}{2}\right) + \varepsilon\left\{-\frac{A}{16}\left[\cos(5t + \tfrac{3}{2}k\pi) + 2\cos\left(3t + \frac{k\pi}{2}\right) + 2\cos\left(t - \frac{k\pi}{2}\right)\right] + \frac{A^3}{64}\left[\tfrac{2}{3}\cos(7t + \tfrac{5}{2}k\pi) + 3\cos(5t + \tfrac{3}{2}k\pi) + 2\cos(3t + \tfrac{5}{2}k\pi) + 5\cos\left(3t + \frac{k\pi}{2}\right) - 3\cos\left(t - \frac{k\pi}{2}\right)\right]\right\} + O(\varepsilon^2). \tag{29}$$

In the case $\omega \cong 1/2$, using a similar analysis, we also develop the expansions to order ε^2 and obtain the following results for the periodic orbits of period 4π:

$$\omega^2 = \frac{1}{4} + \frac{\varepsilon}{8}A^2 - \varepsilon^2\left[\frac{1}{6} - \frac{A^2}{2} + \frac{65}{256}A^4\right] + O(\varepsilon^3), \tag{30a}$$

$$\omega^2 = \frac{1}{4} - \frac{\varepsilon}{8}A^2 - \varepsilon^2\left[\frac{1}{6} - \frac{A^2}{2} + \frac{65}{256}A^4\right] + O(\varepsilon^3), \tag{30b}$$

and

$$\begin{aligned}\hat{Y}(t) = A\cos\left(\frac{t}{2} + \frac{k\pi}{2}\right) + \varepsilon\Big\{\frac{-A}{12}\Big[2\cos\left(\frac{7}{2}t + \frac{3}{4}k\pi\right) + 3\cos\left(\frac{5}{2}t + \frac{k\pi}{4}\right)\\ - 3\cos\left(\frac{3}{2}t - \frac{k\pi}{4}\right) - 6\cos\left(\frac{t}{2} - \frac{3k\pi}{4}\right)\Big] + \frac{A^3}{96}\Big[3\cos\left(\frac{9}{2}t + \frac{5}{4}k\pi\right)\\ + 12\cos\left(\frac{7}{2}t + \frac{3}{4}k\pi\right) + 14\cos\left(\frac{5}{2}t + \frac{k\pi}{4}\right) - 6\cos\left(\frac{3}{2}t - \frac{k\pi}{4}\right)\\ - 36\cos\left(\frac{t}{2} - \frac{3}{4}k\pi\right)\Big]\Big\} + O(\varepsilon^2).\end{aligned} \tag{31}$$

Equations (30a) and (30b) agree very well with the numerical results of Section 2, see Figs 5b and 2b up to $\varepsilon \lesssim 0.2$. Unlike the $\omega \cong 1$ case, however, the agreement of Eq. (30a) is not as good for $\varepsilon \gtrsim 0.2$, owing to the asymmetric twist of the right-hand-side curve, which would require higher-order terms in Eq. (30a) for a more accurate description.

We now use the above results to obtain by second-order perturbation methods the boundaries of the instability regions of synchronized periodic solutions of Eq. (13) in the ω^2, ε plane for $0 < \varepsilon \lesssim 1$, writing the unperturbed frequency in the form

$$\omega^2 = p^2 + \varepsilon a_1 + \varepsilon^2 a_2 + \cdots, \qquad p = 0, \tfrac{1}{2}, 1, \tfrac{3}{2}, 2, \ldots. \tag{32}$$

We study here the cases $p = 1$ and $p = 1/2$, looking for uniformly valid (in t) solutions of Eq. (13), linearized about its synchronized periodic solution $\hat{Y}(t)$; cf. Eqs. (29) and (31) above. Thus, we set

$$Y(t) = \hat{Y}(t) + z(t), \ z(t) \text{ small}, \tag{33}$$

and linearize Eq. (13), keeping terms up to first order in $z(t)$ to obtain

$$\frac{d^2z}{dt^2} + \omega^2 z(t) + \varepsilon\cos 2t(1 - 3\hat{Y}^2(t))z(t) = 0, \tag{34}$$

which is a Hill's equation in $z(t)$.[16]

Using the standard "multiple-scaling" techniques of perturbation theory,[9,11] we write the solution of Eq. (34) as a series expansion in ε:

$$z(t, \varepsilon) = F_0(t, \tilde{t}) + \varepsilon F_1(t, \tilde{t}) + \varepsilon^2 F_2(t, \tilde{t}) + \cdots \tag{35}$$

where

$$\tilde{t} \equiv \varepsilon t. \tag{36}$$

In the case $p = 1$ with $k = 0$ and $A = 0.5$, substituting from Eqs. (32) and (35) (3.25) into Eq. (34), using Eq. (29), and equating like powers of ε, we obtain linear equations for $F_i(t, \tilde{t})$, $i = 0, 1, 2, \ldots$, which are solved successively at every order, making use of the results of previous orders. Imposing the usual requirement that no inhomogeneous terms arise on the rhs of these equations having the same frequency as that of the homogeneous solutions leads to the following expressions for the boundaries of the instability regions in the (ε, ω^2) plane (see Ref. 9 for details):

$$\omega_-^2 \cong 1 - \frac{1}{8}\varepsilon + \frac{3}{256}\varepsilon^2: \quad \text{left branch,} \tag{37a}$$

$$\omega_+^2 \cong 1 + \frac{1}{2}\varepsilon - \frac{9}{1124}\varepsilon^2: \quad \text{right branch.} \tag{37b}$$

These expressions are plotted in Fig. 6a and are in agreement with results of Section 2 (see, e.g., Fig. 3a, where the values $a = \omega^2 = 0.80674575$, $\varepsilon = 0.5$ *lie outside* the instability region of Fig. 6a).

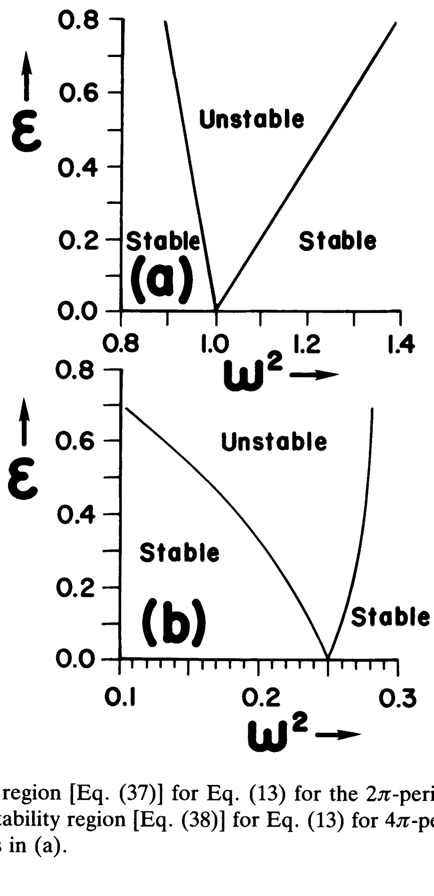

FIGURE 6 (a) Instability region [Eq. (37)] for Eq. (13) for the 2π-periodic solution at $t_0 = 0$, with $y(0) = 0.5$, $\dot{y}(0) = 0$. (b) Instability region [Eq. (38)] for Eq. (13) for 4π-periodic solution at $t_0 = 0$ and the same initial condition as in (a).

By a similar analysis for the case $n = 1/2$, we obtained the following expressions:

$$\omega_-^2 \cong \frac{1}{4} - \frac{3}{32}\varepsilon - \frac{2077}{12{,}288}\varepsilon^2: \text{ left branch,} \tag{38a}$$

$$\omega_+^2 \cong \frac{1}{4} + \frac{2}{32}\varepsilon - \frac{901}{12{,}288}\varepsilon^2: \text{ right branch.} \tag{38b}$$

Again, these expressions are plotted in Fig. 6b and are in agreement with the results of Section 2 (see, e.g., Fig. 4a, where the values $a = \omega^2 = 0.2359465$, $\varepsilon = 0.6$ *lie inside* the instability region of Fig. 6b).

We have also checked the predictions of Eqs. (37) and (38) displayed graphically in Figs. 6a and 6b against numerical computations in many other cases and have found very satisfactory agreement for several values of a, ε (or ω^2, ε) beyond the ones mentioned above. Thus, having demonstrated the validity and usefulness of these methods in the one-dimensional case, we now proceed to apply them in the next section to the case of *two* coupled nonlinear oscillators.

4. SYNCHRONIZED PERIODIC ORBITS IN TWO DIMENSIONS

In this section, we make the first steps towards applying the methods of this paper to study synchronized periodic orbits of two coupled differential equations of the form of Eq. (8):

$$\begin{aligned} \frac{d^2x}{dt^2} + a_1 x + \varepsilon P(t) F_1(x, y) &= 0 \\ \frac{d^2y}{dt^2} + a_2 y + \varepsilon P(t) F_2(x, y) &= 0, \end{aligned} \tag{39}$$

where again $P(t) = P(t + 2\pi)$, $F_i(x, y)$, $i = 1, 2$, are nonlinear functions of x, y, and ε is a small parameter.

As an application to the two-dimensional beam–beam interaction problem, we will, in fact, take $P(t)$ in Eq. (39) to be the 2π-periodic delta function [1–6]

$$P(t) = \delta_{2\pi}(t) = \frac{1}{2\pi} \sum_{n=-\infty}^{\infty} \cos nt \tag{40}$$

and let x and y denote the horizontal and vertical deflections of a weak beam, colliding head on with a bunched strong beam and experiencing, at every collision, an electromagnetic kick of the form[7]

$$\frac{1}{x} F_1(x, y) = \frac{1}{y} F_2(x, y) = 2\,\frac{1 - \exp\left[-(x^2 + y^2)/2\right]}{x^2 + y^2}. \tag{41}$$

Keeping the leading terms in an expansion of Eq. (41) about the origin ($x = y = 0$) and the first three cosine terms in Eq. (40) we look for synchronized periodic solutions of the system

$$\ddot{x} + Q_1^2 x + \varepsilon(\tfrac{1}{2} + \cos t + \cos 2t + \cos 3t)\left(x - \frac{x(x^2+y^2)}{4}\right) = 0 \qquad (42a)$$

$$\ddot{y} + Q_2^2 y + \varepsilon(\tfrac{1}{2} + \cos t + \cos 2t + \cos 3t)\left(y - \frac{y(x^2+y^2)}{4}\right) = 0, \qquad (42b)$$

where Q_1, Q_2 are the machine tunes in the x and y direction, respectively, and ε is a measure of the strength of the beam–beam interaction.

When $\varepsilon = 0$, the general solutions of Eq. (42) are

$$x = a_1 \cos(Q_1 t + \phi_1),\ \dot{x} = -a_1 Q_1 \sin(Q_1 t + \phi_1), \qquad (43a)$$

$$y = a_2 \cos(Q_2 t + \phi_2),\ \dot{y} = -a_2 Q_2 \sin(Q_2 t + \phi_2), \qquad (43b)$$

where a_1, a_2, ϕ_1, ϕ_2 are constants determined by the initial conditions. However, for $\varepsilon \neq 0$, we shall let $a_i(t)$ and $\phi_i(t)$ be functions of time and proceed to determine them by the methods of generalized averaging, described in Section 3.

To this end, we differentiate x and equate with $\dot{x}$ in Eq. (43a) and then differentiate $\dot{x}$ and substitute into Eq. (42a). Doing the same for y, we get a system of equations, which we solve for $\dot{a}_i(t)$, $\dot{\phi}_i(t)$, $i = 1, 2$ to obtain

$$\frac{d}{dt}\begin{bmatrix} a_1(t) \\ a_2(t) \\ \phi_1(t) \\ \phi_2(t) \end{bmatrix} = \frac{\varepsilon}{4}\begin{bmatrix} a_1 S_1 \\ a_2 S_2 \\ S_3 \\ S_4 \end{bmatrix} - \frac{\varepsilon}{64}\begin{bmatrix} a_1^3 R_1 \\ a_2^3 R_2 \\ a_1^2 R_3 \\ a_2^2 R_4 \end{bmatrix} - \frac{\varepsilon}{64}\begin{bmatrix} a_1 a_2^2 T_1 \\ a_1^2 a_2 T_2 \\ a_2^2 T_3 \\ a_1^2 T_4 \end{bmatrix}, \qquad (44)$$

where the S_i, R_i, T_i, $i = 1, 2, 3, 4$, are sums of trigonometric functions with arguments

$$\psi_{j,k} \equiv (2Q_j - k)t + 2\phi_j, \qquad j = 1, 2;\ k = 0,\ \pm 1,\ \pm 2,\ \pm 3 \qquad (45a)$$

(as well as $\cos t$, $\cos 2t$ and $\cos 3t$),coming from the expansions of $\cos^3(Q_1 t + \phi_1)$, $\cos^3(Q_2 t + \phi_2)$, etc.:

$$S_j = \frac{1}{Q_j}\sum_{k=-3}^{3} \sin \psi_{j,k},\ S_{j+2} = \frac{1}{Q_j}\sum_{k=-3}^{3} (\cos \psi_{j,k} + \cos kt),\ j = 1, 2 \qquad (45b)$$

$$\left.\begin{aligned} R_j &= \frac{1}{Q_j}\sum_{k=-3}^{3} [2 \sin \psi_{j,k} + \sin(\psi_{j,0} + \psi_{j,k})] \\ R_{j+2} &= \frac{1}{Q_j}\sum_{k=-3}^{3} [4 \cos \psi_{j,k} + \cos(\psi_{j,0} + \psi_{j,k}) + 3 \cos kt] \end{aligned}\right\} j = 1, 2 \qquad (45c)$$

$$\left.\begin{aligned} T_j &= \frac{1}{Q_j}\sum_{k=-3}^{3} [2 \sin \psi_{j,k} + \sin(\psi_{j,0} \pm \psi_{l,k})] \\ T_{j+2} &= \frac{1}{Q_j}\sum_{k=-3}^{3} [2 \cos \psi_{1,k} + 2 \cos \psi_{2,k} \\ &\quad + \cos(\psi_{j,0} + \psi_{l,k}) + 2 \cos kt]. \end{aligned}\right\} j, l = 1, 2, l \neq j \qquad (45d)$$

Equations (44), with (45), can now be solved by an extension of the techniques of generalized averaging as follows: Write first Eq. (44) in the form

$$\frac{dz}{dt} = \varepsilon f(z, t), \qquad z \equiv [a_1(t), a_2(t), \varphi_1(t), \varphi_2(t)]^t, \tag{46a}$$

(with $[\cdots]^t$ denoting transpose), and let

$$f(z, t) = \bar{f}(u) + \tilde{f}(u, t),$$
$$u \equiv [a_1(t_0), a_2(t_0), \varphi_1(t_0), \varphi_2(t_0)]^t = [A_1, A_2, \Phi_1, \Phi_2]^t, \tag{46b}$$

where the vector functions $\bar{f}(u)$ and $\tilde{f}(u, t)$ contain the terms of smallest frequency (plus constants) and the terms of higher frequency, respectively. As in Section 3, we associate with Eq. (46) the reduced system

$$\frac{du}{dt} = \varepsilon \bar{F}(u), \tag{47a}$$

where

$$z = u + \varepsilon \tilde{G}(u, t). \tag{47b}$$

Cf. Eq. (17b), expand $\bar{F}(u)$, $\tilde{G}(u, t)$ in powers of ε,

$$\bar{F}(u) = \bar{F}_1(u) + \varepsilon \bar{F}_2(u) + \cdots + \varepsilon^{m-1} \bar{F}_m(u) + \cdots \tag{48a}$$
$$\tilde{G}(u, t) = \tilde{G}_1(u, t) + \varepsilon \tilde{G}_2(u, t) + \cdots + \varepsilon^{m-1} \tilde{G}_m(u, t) + \cdots \tag{48b}$$

and substitute from Eq. (48) into Eq. (47), using Eq. (46) (4.8), to obtain, upon equating like powers of ε,

$$\bar{F}_1(u) = \overline{f(u, t)},\ \bar{F}_2(u) = \overline{\frac{\partial \tilde{f}}{\partial u} \int \tilde{f}(u, t)\, dt}, \ldots . \tag{49a}$$

$$\left.\begin{aligned} \tilde{G}_1(u, t) &= \int \tilde{f}(u, t)\, dt \\ \tilde{G}_2(u, t) &= \int \widetilde{\left[\frac{\partial \tilde{f}}{\partial u} \int \tilde{f}(u, t)\, dt\right]} dt + \frac{\partial \bar{f}}{\partial u} \int \left[\int \tilde{f}(u, t)\, dt\right] dt \\ &\quad - \bar{f}\left\{\int \left[\int \frac{\partial \tilde{f}}{\partial u}(u, t)\, dt\right] dt\right\}, \ldots \end{aligned}\right\} \tag{49b}$$

cf. Eq. (19). Moreover, the approximate formulas for the amplitudes and phases of solutions are written as

$$\left.\begin{aligned} a_i(t) &= A_i + \varepsilon \tilde{G}_{1a_i}(u, t) + \varepsilon^2 \tilde{G}_{2a_i}(u, t) + O(\varepsilon^3) \\ \phi_i(t) &= \Phi_i + \varepsilon \tilde{G}_{i\phi_i}(u, t) + \varepsilon^2 \tilde{G}_{2\phi_i}(u, t) + O(\varepsilon^3) \end{aligned}\right\} i = 1, 2 \tag{50}$$

with

$$\tilde{G}_k(u, t) \equiv [\tilde{G}_{ka_1}, \tilde{G}_{ka_2}, \tilde{G}_{k\phi_1}, \tilde{G}_{k\phi_2}]^t, \qquad k = 1, 2.$$

Now, Eq. (44) [with Eq. (45)] is split in such a way that small-frequency components occur at

$$Q_i \cong 1/2,\ 1,\ 3/2,\ 1/4,\ 3/4, \qquad i = 1, 2, \tag{51}$$

and

$$Q_1 \pm Q_2 \cong 1/2,\ 1,\ 3/2$$

and yield terms that contribute to order ε, cf. Eq. (45). Thus, choosing

$$Q_1 \cong 3/4, \qquad Q_2 \cong 1/2 \tag{52}$$

and inserting Eq. (50) into Eq. (44), we obtain the reduced system

$$\frac{d}{dt}\begin{bmatrix} A_1 \\ A_2 \\ \phi_1 \\ \phi_2 \end{bmatrix} = \frac{\varepsilon}{4}\begin{bmatrix} 0 \\ \dfrac{A_2}{Q_2}\sin\psi_{2,1} \\ 1/Q_1 \\ \dfrac{1}{Q_2}(\cos\psi_{2,1}+1) \end{bmatrix} - \frac{\varepsilon}{64}\begin{bmatrix} (A_1^3/Q_1)\sin(\psi_{1,1}+\psi_{1,2}) \\ \dfrac{A_2^3}{Q_2}[2\sin\psi_{2,1}+\sin 2\psi_{2,1}] \\ \dfrac{A_1^2}{Q_1}[\cos(\psi_{1,1}+\psi_{1,2})+3] \\ \dfrac{A_2^2}{Q_2}[4\cos\psi_{2,1}+\cos 2\psi_{2,1}+3] \end{bmatrix}$$

$$-\frac{\varepsilon}{64}\begin{bmatrix} 0 \\ (2A_1^2A_2/Q_2)\sin\psi_{2,1} \\ (2A_2^2/Q_1)(\cos\psi_{2,1}+1) \\ (2A_1^2/Q_2)(\cos\psi_{2,1}+1) \end{bmatrix} = \varepsilon\bar{F}_1(u). \tag{53}$$

To satisfy the conditions $dA_1/dt = dA_2/dt = 0$, we make the corresponding contributions of $\bar{F}_1(u)$ vanish by setting

$$\left.\begin{aligned} \psi_{2,1} &= (2Q_2-1)t + 2\Phi_2 = l\pi \\ \psi_{1,1}+\psi_{1,2} &= (4Q_1-3)t + 4\Phi_1 = m\pi \end{aligned}\right\} l,\ m = 0, 1, 2, \ldots, \tag{54}$$

whence

$$\frac{d\Phi_1}{dt} = -Q_1 + \frac{3}{4}, \qquad \frac{d\Phi_2}{dt} = -Q_2 + \tfrac{1}{2}. \tag{55}$$

Putting all of the above in Eq. (53), we arrive at the following expressions for Q_1^2 and Q_2^2 to first order in ε:

$$\begin{aligned} Q_1^2 &= \frac{9}{16} - \frac{\varepsilon}{2} + \frac{\varepsilon}{32}\{A_1^2[(-1)^m+3] + 2A_2^2[(-1)^l+1]\} + O(\varepsilon^2) \\ Q_2^2 &= \frac{1}{4} - \frac{\varepsilon}{2}[(-1)^l+1] + \frac{\varepsilon}{16}[2A_2^2 + A_1^2][(-1)^l+1] + O(\varepsilon^2). \end{aligned} \tag{56}$$

For different values of l, $m = 0, 1$ we pick different "branches" in the Q_1^2, ε and Q_2^2, ε planes, along which synchronized periodic solutions of Eq. (39) can be found, cf. Eqs. (26) and (30), with initial conditions $\hat{x}(t_1) = A_1$, $\hat{y}(t_2) = A_2$, and $\dot{\hat{x}}(t_1) = \dot{\hat{y}}(t_2) = 0$. These solutions have a periodic $\hat{x}(t)$ component, with period $T_1 = 8\pi/3$, and periodic $\hat{y}(t)$ with period $T_2 = 4\pi$. Their overall period, therefore, is $T = 3T_1 = 2T_2 = 8\pi$.

We have verified the validity of these results by integrating the equations of motion [Eq. (42)] numerically with $\varepsilon = 0.1$ and Q_1, Q_2 chosen from Eq. (56), with $m=0$ and $l=0$. Starting with initial conditions $A_1=0.5$ and $A_2=0.5$, we indeed obtained an 8π-periodic orbit with its $\hat{x}(t)$ and $\hat{y}(t)$ components oscillating with periods of $8\pi/3$ and 4π, respectively, as expected from the above analysis. Furthermore, we find, using Eq. (56), that the particular resonance, $m_1Q_1+m_2Q_2=n$, corresponding to this orbit is $2Q_1-Q_2=1$.

Another interesting low-order resonance, $4m_1=3$, can be studied starting with small initial y values, e.g. $y(0)=1\times10^{-6}$, $\dot{y}(0)=0$. For $x(0)$, $\dot{x}(0)$ not too large, the amplitude of the y oscillations remains small, while the interactions of the orbit with the x, $\dot{x}$ plane, at $t_n=2n\pi$, clearly show the presence of a major stable—and one unstable—period-4 resonance, see Fig. 7. These resonances, and the general features of the motion around them, are highly reminiscent of the pictures one gets by iterating analogous *mapping models* of colliding beams,[1,4,5] which illustrates a general consistency between differential and *difference* equation approaches to the problem of the beam–beam interaction.

Currently, we are in the process of studying analytically and numerically the *stability* of the synchronized periodic solutions of Eq. (42) obtained in this section. This is considerably more complicated than the one-dimensional case of Sections 2 and 3; here, the corresponding variational problem involves *coupled* Hill's type equations, for which the general theory is not readily available. Still, multiple scaling techniques are expected to apply, and numerical experiments can be performed to study the regions of stability about these important periodic orbits, after they have first been found by the methods of this paper.

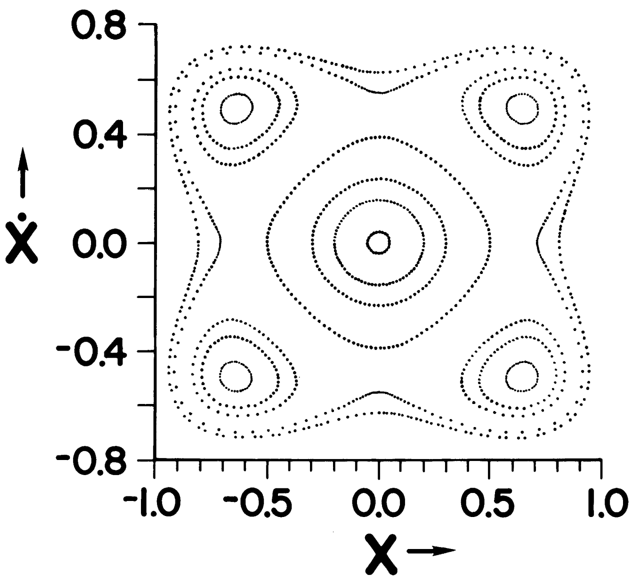

FIGURE 7 Orbit intersections of solutions of Eq. (42) with the x, $\dot{x}$ plane for $\varepsilon=0.1$, $Q_1^2=0.51875$, $Q_2^2=0.25$, $y(0)=1\times10^{-6}$; $\dot{y}(0)=0$. Note the presence of a period-4 resonance, in this quasi-one-dimensional case. The y oscillations here remain small ($\sim10^{-5}$) for all t.

Finally, we intend to include in our models the effects of synchrotron (or, longitudinal) oscillations,[1–3] which we have entirely neglected here. These oscillations are known to couple with the x, y motion of the particles and create *new* resonances, which further enhance beam blow up and compound the instabilities of the beam–beam interaction.

ACKNOWLEDGMENTS

This work was supported in part by the DOE., Division of High Energy Physics, under grant no. DE-FG02-83ER40144.A002. We wish to thank Dr. David Sutter for many helpful discussions and comments.

REFERENCES

1. M. Month and J. C. Herrera, Eds., *Nonlinear Dynamics and the Beam–Beam Interaction,* AIP Conf. Proc. No. 57, (AIP, New York 1979).
2. *Physics of High Energy Accelerators,* Fermi-lab Summer School 1981 Proceedings, R. A. Carrigan, F. R. Huson and M. Month, Eds. AIP Conf. Proc. No. 87, (AIP, New York 1982).
3. Workshop on Orbital Dynamics in High Energy Accelerators, March 7-12, 1985; *Particles Accelerators* **19** (1986).
4. T. Bountis C. R. Eminlizer and R. H. G. Helleman, in *Long Time Prediction in Dynamics,* W. Horton, L. Reichl and V. Szebehely, Eds. (J. Wiley, New York 1982).
5. T. Bountis, C. R. Eminlizer and N. Budinsky, *Nucl. Inst. Meth,* **227,** 205 (1984).
6. T. Bountis, in Ref. 3.
7. See e.g. J. Herrera's article in Ref. 1.
8. G. Mahmoud, T. Bountis "Synchronized Periodic Solutions of a Class of Periodically Driven Nonlinear Oscillators", submitted to *Journ. Appl. Mech.*
9. T. Bountis & E. Coutsias, in Ref. 1.
10. J. Haag, *Oscillatory Motions,* (Wadsworth Publ. Balmont, CA, 1962); see also N. N. Bogoliubov and Y. A. Mitropolsky, *Asymptotic Methods in the Theory of Nonlinear Oscillations,* (Gordon and Breach, New York, 1961).
11. A. H. Nayfeh and D. T. Mook, *Nonlinear Oscillations* (Wiley, New York, 1979).
12. M. Abramowitz and I. Stegun, *Handbook of Mathematical Functions,* Chapt. 20, (Dover, New York, 1965).
13. M. Lieberman and A. Lichtenberg, *Regular and Stochastic Motion,* (Springer Verlag, New York, 1983).
14. M. V. Berry, in *Topics in Nonlinear Dynamics,* ed. S. Jorna, Ed., AIP conf. Proc. Vol. 46 (AIP New York, 1978).
15. R. H. G. Helleman in *Fundamental Problems in Statistical Mechanics* Vol. 5, E. G. D. Cohen, Ed. (North Holland, Amsterdam 1981).
16. W. Magnus and S. Winkler, *Hill's Equation,* (Interscience, New York, 1966).